PHYSICAL REVIEW B VOLUME 8, NUMBER 6 15 SEPTEMBER 1973

Spherical Model of Shallow Acceptor States in Semiconductors

A. Baldereschi*
Bell Laboratories, Murray Hill, New Jersey 07974

Nunzio O. Lipari
Xerox Research Laboratories, Rochester, New York 14644
(Received 13 March 1973)

The effective-mass approximation for shallow acceptor states in cubic semiconductors with degenerate valence bands is reformulated. The Hamiltonian is written as the sum of a spherical term and a cubic correction, thus pointing out the relevance of the spherical symmetry in the acceptor problem and the strong similarity to the case of atoms with the spin-orbit interaction. Without the introduction of any explicit representation of the Hamiltonian, the present formulation yields a meaningful classification of the acceptor states and reduces the eigenvalue problem to simple radial Hamiltonians. These radial Hamiltonians are explicitly given for the most improtant acceptor states and are shown to apply also to the description of the exciton problem. The variational metlod is used in the numerical calculation. The resulting eigenvalues, eigenfunctions, and related quantities are given as functions of the relevant parameters. The theoretical ionization energies are compared with available experimental data.

I. INTRODUCTION

The optical and transport properties of semiconductors are strongly affected by the presence of charged impurities, owing to the bound states that such impurities produce in the forbidden energy gap.[1] Depending on its valence being larger or smaller than that of the host atom it replaces, the impurity can act as a donor or acceptor, respectively. In the former case, the extra electrons are associated with the conduction-band minimum whereas, in the latter, the missing electrons (holes) are related to the valence-band maximum.

The relation between impurity states and band structure has been studied by Kittel and Mitchell[2] and Luttinger and Kohn,[3] within the limits of the effective-mass approximation. The potential produced by charged impurities is long range. At distances from the impurity site large compared to the lattice constant, this potential is well described by a Coulomb potential screened by the dielectric constant of the host. At distances smaller than or comparable to the lattice constant, the potential strongly deviates from the Coulombic behavior because of the presence of the impurity core. Since the wave functions of these bound states generally extend over distances of many lattice constants, the deviations affect only the ground state (central-cell corrections).

Donors and acceptors have been most studied[4] in crystals with the diamond and zinc-blende lattice. For these substances, it is well known[5] that the band structure has a simple minimum in the conduction band and a degenerate maximum in the valence band. Therefore donor states are easily investigated[6,7] whereas a complex analysis is required for acceptor states.[8-12]

The first investigation of acceptors in Si and Ge was done by Kohn and Schecter.[8] Using the variational method, they calculated the energies of the lowest four optical transitions in the acceptor spectrum. Later Mendelson and James[9] considered again the acceptor spectrum of Ge using the same variational approach but with more general trial functions. Since then, Suzuki *et al.*[10] and Mendelson and Schultz[11] have improved the previous variational calculations by including the split-off valence band, whereas Sheka and Sheka[12] have included the lowest conduction band in order to treat the case of small-gap semiconductors.

All these calculations show that the effective-mass approximation is satisfactory for excited states whereas, for the ground state, one must consider the chemical shift. These investigations, which use a brute force variational approach, have not helped in achieving a clear insight of the acceptor spectrum. In particular, these results do not show explicitly the dependence of the acceptor spectrum on the energy-band parameters and therefore they cannot be generalized to any cubic semiconductor. Furthermore, these calculations are time consuming even when a small number of trial wave functions is used; and the limited number (i.e., two) of angular momenta represented in the trial functions has no justification but necessity.

Recently, we have given preliminary reports[13] of a new approach to the acceptor problem which has several advantages over the previous investigations: The simple formulation of the problem and the absence of any explicit representation of the Hamiltonian make possible a clear insight and a meaningful classification of the acceptor states. Furthermore the new formulation suggests a new set of parameters to describe the valence band,

which allow us to tabulate results for any cubic semiconductor. In order to achieve all these advantages we make use of the strong similarity between acceptor centers and atomic and nuclear systems. This similarity, which has not been fully exploited so far, becomes apparent from the acceptor Hamiltonian if the terms which have strict cubic symmetry are separated from the terms which, besides having cubic symmetry, are also spherically symmetric. Since the former terms generally contribute much less to binding than the latter terms, we can neglect the cubic contribution in first approximation. In this way, we are left with a spherical model of the acceptor center which is strongly similar to atomic systems with the spin-orbit interaction included. In this analogy, different degenerate valence bands in the acceptor case play the role of different spin states in the atomic counterpart. Large profit can be obtained from this similarity because we can use the theorems and techniques of the angular momentum theory which were very useful in the study of atomic systems. The effect of the cubic term may then be added as a perturbation of the spherical model.

The spherical model is presented in detail in Sec. II. The radial Hamiltonians which describe acceptor states of various symmetries are derived in Sec. III in the limits of strong and weak spin-orbit coupling. Section IV is devoted to the numerical solution of these Hamiltonians. In this section we give the results for the acceptor energy levels, wave functions, mean radii, and probability to be in the central cell (the latter quantity is useful in the evaluation of central-cell corrections). The admixture coefficients of different angular momenta in the acceptor wave functions are also given to show the effect of interband coupling in this problem. Furthermore, the theoretical energy spectrum of acceptors is explicitly given for several semiconductors and compared with available experimental data. In Sec. V we summarize the main achievements of the present work and discuss possible extensions. For convenience, in the Appendix we give the concepts and theorems of angular momentum theory which are used in the present paper.

II. SPHERICAL MODEL

In the present paper the acceptor center is described with a Coulomb potential screened by the static dielectric constant of the host crystal. Previous investigations[8–11] have shown that this approximation is satisfactory for excited states but not for the ground state, whose binding energy is affected by central-cell corrections due to the impurity core. We feel, however, that accurate solutions of the acceptor problem in the Coulomb approximation are nevertheless of great interest even for the ground state since they allow an estimate of the magnitude of central-cell corrections. Furthermore we will restrict ourselves to the more common case of singly charged acceptors because this is the case where central-cell effects are less relevant. In fact, the larger the charge, the more localized (and therefore sensitive to chemical shifts) are the acceptor wave functions. Assuming also that the acceptor kinetic energy is well described in the effective-mass approximation, the acceptor Hamiltonian is[14]

$$H=(\gamma_1+\tfrac{5}{2}\gamma_2)\frac{p^2}{2m_0}-\frac{\gamma_2}{m_0}(p_x^2J_x^2+p_y^2J_y^2+p_z^2J_z^2)$$
$$-\frac{2\gamma_3}{m_0}[\{p_xp_y\}\{J_xJ_y\}+\{p_yp_z\}\{J_yJ_z\}$$
$$+\{p_zp_x\}\{J_zJ_y\}]-\frac{e^2}{\epsilon_0 r}, \quad (1)$$

where $\{ab\}=(ab+ba)/2$; ϵ_0 and m_0 are the crystal dielectric constant and the free electron mass, respectively; γ_1, γ_2, and γ_3 are the parameters proposed by Luttinger for the description of the hole dispersion relation near the center of the Brillouin zone; $\vec{p}$ is the hole linear momentum operator and $\vec{J}$ is the angular momentum operator corresponding to spin $\frac{3}{2}$. Hamiltonian (1) is valid for crystals with the diamond structure and in the limit of strong spin-orbit coupling, i.e., when the valence-band spin-orbit splitting Δ at the center of the Brillouin zone is much larger than the acceptor binding energy. In the case of zinc-blende crystals, terms linear in $\vec{p}$ should be added to Hamiltonian (1) but, as we have already proved in the case of exciton states, [15] the binding contribution due to these terms is very small and therefore negligible.

The above Hamiltonian can be thought of as describing a particle with spin $\frac{3}{2}$ in a Coulomb potential. The first term is the particle kinetic energy, the second and third terms represent a kind of "spin-orbit" interaction, and the last term is the external potential. The strong analogy with atomic systems is evident. In the study of Hamiltonian (1) it is therefore convenient to use the same techniques which have been successfully applied in the theory of atomic spectra. To begin, let us introduce the following second-rank Cartesian tensor operators[12]:

$$P_{ik}=3p_ip_k-\delta_{ik}p^2 \quad (2a)$$

and

$$J_{ik}=\tfrac{3}{2}(J_iJ_k+J_kJ_i)-\delta_{ik}J^2, \quad (2b)$$

where the indices i, $k=1$, 2, 3 mean x, y, z, respectively. These operators are symmetric tensors

$$P_{ik}=P_{ki} \text{ and } J_{ik}=J_{ki} \quad (3)$$

which have vanishing trace

$$P_{ik}\delta_{ik}=0 \quad \text{and} \quad J_{ik}\delta_{ik}=0, \tag{4}$$

where we have used the Einstein convention on repeated indices. The convenience of introducing the tensor operators P_{ik} and J_{ik} is due to the fact that the operators $\vec{p}$ and $\vec{J}$ appear in Hamiltonian (1) in second order only. With the help of these tensor operators, the acceptor Hamiltonian can be written in compact form as follows:

$$H=\frac{\gamma_1}{2m_0}p^2-\frac{e^2}{\epsilon_0 r}-\frac{1}{9m_0}[\gamma_3-(\gamma_3-\gamma_2)\delta_{ik}]P_{ik}J_{ik}. \tag{5}$$

The Cartesian tensors (2a) and (2b) are reducible tensors of second rank and therefore they can be decomposed into irreducible spherical tensors of rank $l=0$, 1, and 2. Because of the symmetry property (3) such decomposition does not contain the $l=1$ component. Since also the $l=0$ component is absent because our tensors have vanishing trace, we can write Hamiltonian (5) in terms of the second-rank ($l=2$) irreducible components $P_q^{(2)}$ and $J_q^{(2)}$ ($q=-2,\ -1,\ 0,\ 1,\ 2$) as follows:

$$H=\left(\frac{\gamma_1}{2m_0}p^2-\frac{e^2}{\epsilon_0 r}\right)-\frac{3\gamma_3+2\gamma_2}{45m_0}(P^{(2)}\cdot J^{(2)}) +\frac{\gamma_3-\gamma_2}{18m_0}\{[P^{(2)}\times J^{(2)}]_{-4}^{(4)}+\tfrac{1}{5}\sqrt{70}[P^{(2)}\times J^{(2)}]_0^{(4)} +[P^{(2)}\times J^{(2)}]_4^{(4)}\}, \tag{6}$$

where we have used the definitions of scalar and vector products of irreducible spherical tensor operators which are given in the Appendix.

Expressions (1) and (6) are different but equivalent ways of writing the same acceptor Hamiltonian. The symmetry of our problem is obviously cubic and according to symmetry considerations Luttinger[14] wrote Hamiltonian (1) as the most general expression in second order in $\vec{p}$ and with cubic symmetry. Expression (6) is equivalent to (1) but is written in terms of spherical tensors which are irreducible representations of the full rotation group and not of the cubic point group of the crystal. This makes it possible to separate in (6) the last term, which is strictly cubic, from the first two, which, besides having cubic symmetry, are also spherically invariant. This separation of the acceptor Hamiltonian into terms with spherical and cubic symmetry is the foundation of the spherical model that we are going to present. The rearrangement of terms in (6) suggests a more convenient set of parameters for the description of the acceptor problem. Together with γ_1, we use the parameter

$$\mu=(6\gamma_3+4\gamma_2)/5\gamma_1, \tag{7}$$

which gives the strength of the spherical spin-orbit interaction, i.e., the second term in (6), and the parameter

$$\delta=(\gamma_3-\gamma_2)/\gamma_1, \tag{8}$$

which measures the cubic contribution, i.e., the last term in (6). Furthermore we use the effective Rydberg

$$R_0=e^4m_0/2\hbar^2\epsilon_0^2\gamma_1 \tag{9}$$

and the effective Bohr radius

$$a_0=\hbar^2\epsilon_0\gamma_1/e^2m_0 \tag{10}$$

as units of energy and length, respectively, and we write Hamiltonian (6) as follows:

$$H=\frac{1}{\hbar^2}p^2-\frac{2}{r}-\frac{1}{9\hbar^2}\mu(P^{(2)}\cdot J^{(2)}) +\frac{1}{9\hbar^2}\delta\{[P^{(2)}\times J^{(2)}]_4^{(4)} +\tfrac{1}{5}\sqrt{70}[P^{(2)}\times J^{(2)}]_0^{(4)}+[P^{(2)}\times J^{(2)}]_{-4}^{(4)}\}, \tag{11}$$

where the band structure of the host crystal is characterized through the valence-band parameters μ and δ.

The values of the parameters μ and δ for 13 crystals with the diamond and zinc-blende structure are listed in Table I together with the Luttinger valence-band parameters γ_1, γ_2, and γ_3 and the values of the dielectric constant ϵ_0. From these values it is evident that, with the only exception of Si for which $\mu/\delta\approx 2$, the parameter δ is much smaller than the parameter μ, and therefore the cubic term in Hamiltonian (11) will contribute little to the binding energy.[13] In the present paper we will completely neglect the cubic term in (11) and we will study the acceptor problem in the spherical approximation which is described by the following Hamiltonian:

$$H_{sph}=(1/\hbar^2)[p^2-\tfrac{1}{9}\mu(P^{(2)}\cdot J^{(2)})]-2/r, \tag{12}$$

which has full rotational symmetry. The effects of the cubic term will be studied in a future paper[16] as a perturbation on the solutions of (12).

The valence-band energy dispersion relation is given in the spherical model by

$$E=-(\gamma_1/2m_0)p^2-\tfrac{1}{9}\mu(P^{(2)}\cdot J^{(2)}), \tag{13}$$

where $\vec{p}=\hbar\vec{k}$ is a c number. Considering that J is the angular momentum operator corresponding to spin $\frac{3}{2}$, we can solve (13) and find two parabolic bands with curvature independent of the direction of $\vec{k}$,

$$E_\pm=-(\hbar^2\gamma_1/2m_0)(1\pm\mu)k^2. \tag{14}$$

The dispersion relation (14) is represented in Fig. 1 for different values of μ. Note that the parameter μ has been defined in such a way that for $\mu=1$ one of the two bands becomes flat. Furthermore, for values of μ larger than 1, the spherical model

TABLE I. Values of the static dielectric constant ϵ_0 and of the valence- band parameters γ_1, γ_2, and γ_3 used in the present calculation. The valence-band parameters μ and δ introduced in the present paper in connection with the spherical model are also given together with the energy and length units R_0 and a_0, respectively.

	ϵ_0	γ_1[a]	γ_2[a]	γ_3[a]	μ	δ	R_0 (meV)	a_0(Å)
Si	11.40[b]	4.22	0.39	1.44	0.483	0.249	24.8	25.5
Ge	15.36[b]	13.35	4.25	5.69	0.766	0.108	4.3	108.5
AlSb	12.0[c]	4.15	1.01	1.75	0.701	0.178	22.8	26.4
GaP	10.75[d]	4.20	0.98	1.66	0.661	0.162	28.0	23.9
GaAs	12.56[e]	7.65	2.41	3.28	0.767	0.114	11.3	50.8
GaSb	15.7[c]	11.80	4.03	5.26	0.808	0.104	4.7	98.0
InP	12.4[f]	6.28	2.08	2.76	0.792	0.108	14.1	41.2
InAs	14.6[g]	19.67	8.37	9.29	0.907	0.047	3.2	152.0
InSb	17.9[c]	35.08	15.64	16.91	0.935	0.036	1.2	332.3
ZnS	8.1[h]	2.54	0.75	1.09	0.751	0.134	81.6	10.9
ZnSe	9.1[h]	3.77	1.24	1.67	0.795	0.114	43.6	18.2
ZnTe	10.1[h]	3.74	1.07	1.64	0.755	0.152	35.7	20.0
CdTe	9.7[h]	5.29	1.89	2.46	0.844	0.108	27.3	27.2

[a]For valence-band parameters see P. Lawaetz, Phys. Rev. B 4, 3460 (1971).
[b]R. A. Faulkner, Phys. Rev. 184, 713 (1969).
[c]M. Hass and B. W. Henvis, J. Phys. Chem. Solids 23, 1099 (1962).
[d]L. Patrick and P. J. Dean, Phys. Rev. 188, 1254 (1969).
[e]G. E. Stillman, D. M. Larsen, C. M. Wolfe, and R. C. Brandt, Solid State Commun. 9, 2245 (1971).
[f]C. Hilsum, S. Fray, and C. Smith, Solid State Commun. 7, 1057 (1969).
[g]O. G. Lorimor and W. G. Spitzer, J. Appl. Phys. 36, 1841 (1965).
[h]D. Berlincourt, H. Jaffe, and L. R. Shiozawa, Phys. Rev. 129, 1009 (1963).

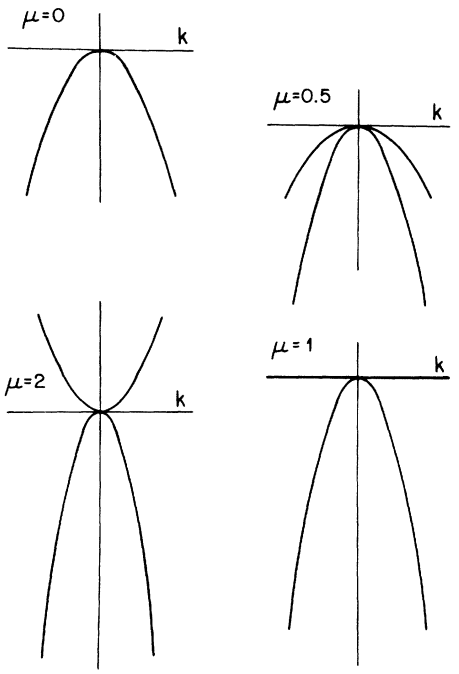

FIG. 1. Energy dispersion relation for the top four valence bands near the center of the Brillouin zone as described by the spherical model. Each band is doubly degenerate. Note that for $\mu=1$ one valence band becomes flat and that for $\mu>1$ the spherical model describes the inverted-valence-band structure.

describes the dispersion relation characteristic of narrow-gap semiconductors like α-Sn and the mercury compounds. The more general dispersion relation corresponding to Hamiltonian (1) and including also the cubic contributions is easily shown to be

$$E'_{\pm} = -(\hbar^2\gamma_1/2m_0)\{k^2 \pm [(\mu - \tfrac{6}{5}\delta)^2 k^4 + \tfrac{12}{5}\delta(5\mu - \delta)(k_x^2k_y^2 + k_y^2k_z^2 + k_z^2k_x^2)]^{1/2}\}, \quad (15)$$

which for $\delta = 0$ reduces to (14). The effects of the approximations involved in the spherical model, i.e., of replacing the dispersion relation (15) with the more simple expression (14), are shown in Fig. 2 for Ge, which represents a typical case as can be seen from the values given in Table I. According to the dispersion relation (15) the curvature of the two parabolic bands depends on the direction of $\vec{k}$. From Fig. 2 we see, however, that such dependence is quite small for common values of δ, and this is the reason of the soundness of the spherical model.

The spherical-model Hamiltonian (12) is valid in the limit of strong spin-orbit coupling between the valence bands. We also wish to study the opposite limiting case, i.e., the case of vanishing spin-orbit coupling. Even though this latter case occurs less frequently than the former, nevertheless its study will be useful in estimating the effect of the spin-orbit interaction on the acceptor binding

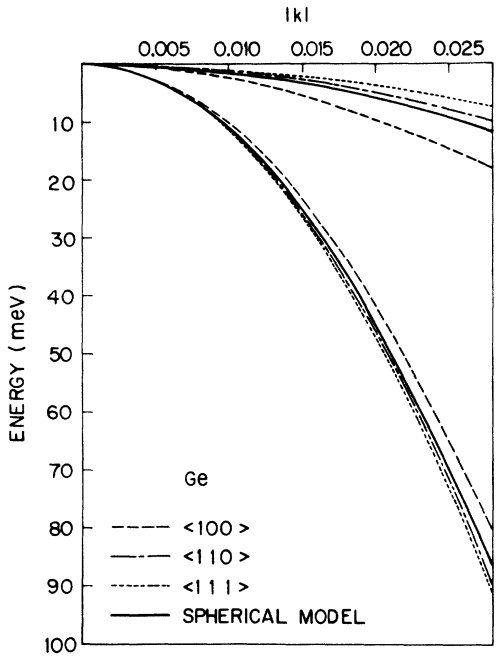

FIG. 2. Actual energy dispersion relation for the valence bands of Ge near the center of the Brillouin zone and along the main symmetry directions Δ, Σ, and Λ. The deviations between the real valence bands and those predicted by the spherical model (also shown) are produced by the cubic term.

energy. Neglecting spin and the spin-orbit interaction, the valence band is threefold degenerate at the center of the Brillouin zone and the acceptor Hamiltonian corresponding to (1) is[14]

$$H' = (\gamma_1 + 4\gamma_2)\frac{p^2}{2m_0} - \frac{3\gamma_2}{m_0}(p_x^2 I_x^2 + p_y^2 I_y^2 + p_z^2 I_z^2) - \frac{6\gamma_3}{m_0}[\{p_x p_y\}\{I_x I_y\} + \{p_y p_z\}\{I_y I_z\} + \{p_z p_x\}\{I_z I_x\}], \quad (16)$$

which is very similar to (1) except for numerical constants and the fact that the operator J is replaced by I, the angular momentum operator corresponding to spin 1. We define in analogy with (2b) the Cartesian tensor

$$I_{ik} = \tfrac{3}{2}(I_i I_k + I_k I_i) - \delta_{ik} I^2, \quad (17)$$

which has the same properties (3) and (4) of the tensor J_{ik}. Using the second-rank irreducible components $I_q^{(2)}$ ($q = -2, -1, 0, 1, 2$) of the tensor (17) and using the units (9) and (10) we can write Hamiltonian (16) as follows:

$$H' = \frac{1}{\hbar^2}p^2 - \frac{2}{r} - \frac{1}{3\hbar^2}\mu(P^{(2)}\cdot I^{(2)}) + \frac{1}{3\hbar^2}\delta\{[P^{(2)}\times I^{(2)}]_4^{(4)} + \tfrac{1}{5}\sqrt{70}\,[P^{(2)}\times I^{(2)}]_0^{(4)} + [P^{(2)}\times I^{(2)}]_{-4}^{(4)}\}, \quad (18)$$

which is completely analogous to (11). It is evident that also in this case we can apply the spherical approximation, since the relative strength of the cubic term is similar in (11) and (18). The spherical-model acceptor Hamiltonian in the limit of vanishing spin-orbit interaction can therefore be written as follows:

$$H'_{\rm sph} = (1/\hbar^2)[p^2 - \tfrac{1}{3}\mu(P^{(2)}\cdot I^{(2)})] - 2/r. \quad (19)$$

Before analyzing the spherical-model Hamiltonians (12) and (19), we wish to discuss analogies and differences between the acceptor problem and the direct exciton problem in crystals with the diamond and zinc-blende structure. The Hamiltonian which describes the relative electron-hole motion of direct excitons[15,17] is

$$H_{\rm ex} = H + p^2/2m_e, \quad (20)$$

where H is the acceptor Hamiltonian and m_e is the electron effective mass at the center of the Brillouin zone. Since the second term on the right-hand side of (20) is easily included into the acceptor Hamiltonian H by substituting the parameter γ_1 with $\gamma_1' = \gamma_1 + m_0/m_e$, we see that the acceptor and the exciton Hamiltonians are formally similar. One would be tempted, therefore, to solve the acceptor problem following the same lines used for the exciton problem.[15] Experimental data, however, show that the two kinds of energy spectra are completely different in that the exciton spectrum resembles very closely that of the hydrogen atom whereas the acceptor spectrum is completely different. The solution of this puzzle is evident after writing Hamiltonian (20) in a dimensionless form analogous to (11). Using the units (9) and (10), where γ_1 is replaced by γ_1', we obtain for the exciton Hamiltonian

$$H_{\rm ex} = \frac{1}{\hbar^2}p^2 - \frac{2}{r} - \frac{1}{9\hbar^2}\alpha\mu(P^{(2)}\cdot J^{(2)}) + \frac{1}{9\hbar^2}\alpha\delta\{[P^{(2)}\times J^{(2)}]_4^{(4)} + \tfrac{1}{5}\sqrt{70}[P^{(2)}\times J^{(2)}]_0^{(4)} + [P^{(2)}\times J^{(2)}]_{-4}^{(4)}\}, \quad (21)$$

which is exactly equal to the acceptor Hamiltonian (11) except for the fact that both the spherical and the cubic spin-orbit contributions are scaled by a factor $\alpha = \gamma_1/\gamma_1' = \gamma_1/(\gamma_1 + m_0/m_e)$ whose value is typically of the order 0.3, as shown in Table II.

Even though the exciton and the acceptor spectra are described by the same formal Hamiltonian, the two cases differ considerably because of the different strength of the spin-orbit terms. While in the exciton case these terms can be adequately treated by using perturbation theory, a more sophisticated treatment is necessary for the acceptor spectrum.

TABLE II. Values of the scaling parameter α, which describes the strength ratio of the "spin-orbit" terms in the exciton and in the acceptor Hamiltonians. The scaling parameter is calculated using the values of γ_1 given in Table I and the electron masses quoted in Ref. 15.

Ge	0.34	InAs	0.32
AlSb	0.04	InSb	0.34
GaP	0.35	ZnS	0.50
GaAs	0.34	ZnSe	0.49
GaSb	0.36	ZnTe	0.25
InP	0.32	CdTe	0.34

In Sec. IV we will show that the scaling parameter $\alpha \approx 0.3$ is indeed responsible for the big differences between acceptor and exciton spectra.

III. ANALYSIS OF SPHERICAL-MODEL HAMILTONIAN

In this section we present a qualitative study of the spherical-model Hamiltonians (12) and (19) which are valid in the limits of strong and weak spin-orbit coupling, respectively. These Hamiltonians can be thought of as describing an hydrogen atom perturbed by a spherical term

$$\alpha\mu(P^{(2)}\cdot S^{(2)}) \tag{22}$$

which can be considered as a kind of "spin-orbit" interaction when the spin operator S assumes the values $\frac{3}{2}$ and 1 in the limits of large and small spin-orbit splitting Δ, respectively. For $\mu = 0$, Hamiltonians (12) and (19) become identical to each other and to the hydrogen-atom Hamiltonian and therefore can be solved exactly. For this case the acceptor energy spectrum is given by

$$E(\mu = 0) = -1/n^2 \tag{23}$$

when the energy unit (9) has been used and n is the usual hydrogenic principal quantum number. The eigenstates can be classified according to $n = 1, 2, 3, \ldots$, and to the values of the orbital angular momentum L and its component in any given direction, which we will assume to be the z direction.

For $\mu \neq 0$ we have to consider the "spin" operator $\vec{S}$ and the spin-orbit term (22). The acceptor Hamiltonians (12) and (19) are spherically symmetric in the coupled orbital and spin spaces and the total angular momentum $\vec{F} = \vec{L} + \vec{S}$ is a constant of the motion. Accordingly the acceptor states can be classified following the L-S coupling scheme used for atomic systems. Since for practical purposes the only important acceptor states are those with $L = 0$ and $L = 1$, in what follows we will limit our consideration to them. Furthermore since the L-S coupling scheme depends on the particular value of S, we will distinguish the two cases of strong and weak spin-orbit coupling.

A. Strong Spin-Orbit Coupling

In this case Hamiltonian (12) is valid and the total angular momentum is $\vec{F} = \vec{L} + \vec{J}$. While the hydrogenic nS states give rise only to $nS_{3/2}$ states (the numerical lower index representing the value of F), the hydrogenic nP states split into $nP_{1/2}$, $nP_{3/2}$, and $nP_{5/2}$. Furthermore the spin-orbit term in Hamiltonian (12) couples only hydrogenic states for which $\Delta L = 0, \pm 2$. This selection rule, together with the fact that F is a constant of motion, defines the most general expression for the eigenfunctions of the acceptor Hamiltonian. For the most important acceptor states the most general wave functions can be written as

$$\Phi(S_{3/2}) = f_0(r)\,|L=0,\ J=\tfrac{3}{2},\ F=\tfrac{3}{2},\ F_z\rangle + g_0(r)\,|L=2,\ J=\tfrac{3}{2},\ F=\tfrac{3}{2},\ F_z\rangle, \tag{24a}$$

$$\Phi(P_{1/2}) = f_1(r)\,|L=1,\ J=\tfrac{3}{2},\ F=\tfrac{1}{2},\ F_z\rangle, \tag{24b}$$

$$\Phi(P_{3/2}) = f_2(r)\,|L=1,\ J=\tfrac{3}{2},\ F=\tfrac{3}{2},\ F_z\rangle + g_2(r)\,|L=3,\ J=\tfrac{3}{2},\ F=\tfrac{3}{2},\ F_z\rangle, \tag{24c}$$

$$\Phi(P_{5/2}) = f_3(r)\,|L=1,\ J=\tfrac{3}{2},\ F=\tfrac{5}{2},\ F_z\rangle + g_3(r)\,|L=3,\ J=\tfrac{3}{2},\ F=\tfrac{5}{2},\ F_z\rangle, \tag{24d}$$

where the functions $|L, J, F, F_z\rangle$ are eigenfunctions of the total angular momentum in the L-J coupled scheme and $f_i(r)$ and $g_i(r)$ are general radial functions which are defined by the condition that the functions (24) must be eigenfunctions of the Hamiltonian (12). To calculate the matrix element of the acceptor Hamiltonian between the functions (24), we use the "reduced-matrix-element" technique,[18] which for our purposes can be written

$$\langle L', J, F, M|(P^{(2)}\cdot J^{(2)})|L, J, F, M\rangle = (-1)^{L+J+F}\begin{Bmatrix} F & J & L' \\ 2 & L & J \end{Bmatrix}\times(J||J^{(2)}||J)(L'||P^{(2)}||L), \tag{25}$$

which expresses the matrix element of the spin-orbit term (22) as a function of a 6-j symbol[18] and of the reduced matrix elements $(J||J^{(2)}||J)$ and $(L'||P^{(2)}||L)$ which are explicitly calculated in the Appendix. The matrix element of the hydrogenlike term that appears in (12) is calculated very simply and is

$$\langle L', J, F, M|\frac{1}{\hbar^2}p^2 - \frac{2}{r}|L, J, F, M\rangle = \left[-\frac{1}{r^2}\frac{d}{dr}\left(r^2\frac{d}{dr}\right) + \frac{L(L+1)}{r^2} - \frac{2}{r}\right]\delta_{LL'}. \tag{26}$$

As a result we obtain that the radial wave functions $f_i(r)$ and $g_i(r)$ must be solutions of the following systems of differential equations:

$$\begin{vmatrix} \frac{d^2}{dr^2}+\frac{2}{r}\frac{d}{dr}+\frac{2}{r}-E & -\mu\left(\frac{d^2}{dr^2}+\frac{5}{r}\frac{d}{dr}+\frac{3}{r^2}\right) \\ -\mu\left(\frac{d^2}{dr^2}-\frac{1}{r}\frac{d}{dr}\right) & \frac{d^2}{dr^2}+\frac{2}{r}\frac{d}{dr}-\frac{6}{r^2}+\frac{2}{r}-E \end{vmatrix} \begin{vmatrix} f_0(r) \\ g_0(r) \end{vmatrix} = 0, \tag{27a}$$

$$\left[(1+\mu)\left(\frac{d^2}{dr^2}+\frac{2}{r}\frac{d}{dr}-\frac{2}{r^2}\right)+\frac{2}{r}-E\right] f_1(r) = 0, \tag{27b}$$

$$\begin{vmatrix} (1-\frac{4}{5}\mu)\left(\frac{d^2}{dr^2}+\frac{2}{r}\frac{d}{dr}-\frac{2}{r^2}\right)+\frac{2}{r}-E & -\frac{3}{5}\mu\left(\frac{d^2}{dr^2}+\frac{7}{r}\frac{d}{dr}+\frac{8}{r^2}\right) \\ -\frac{3}{5}\mu\left(\frac{d^2}{dr^2}-\frac{3}{r}\frac{d}{dr}+\frac{3}{r^2}\right) & (1+\frac{4}{5}\mu)\left(\frac{d^2}{dr^2}+\frac{2}{r}\frac{d}{dr}-\frac{12}{r^2}\right)+\frac{2}{r}-E \end{vmatrix} \begin{vmatrix} f_2(r) \\ g_2(r) \end{vmatrix} = 0, \tag{27c}$$

$$\begin{vmatrix} (1+\frac{1}{5}\mu)\left(\frac{d^2}{dr^2}+\frac{2}{r}\frac{d}{dr}-\frac{2}{r^2}\right)+\frac{2}{r}-E & -\frac{2}{5}\sqrt{6}\,\mu\left(\frac{d^2}{dr^2}+\frac{7}{r}\frac{d}{dr}+\frac{8}{r^2}\right) \\ -\frac{2}{5}\sqrt{6}\,\mu\left(\frac{d^2}{dr^2}-\frac{3}{r}\frac{d}{dr}+\frac{3}{r^2}\right) & (1-\frac{1}{5}\mu)\left(\frac{d^2}{dr^2}+\frac{2}{r}\frac{d}{dr}-\frac{12}{r^2}\right)+\frac{2}{r}-E \end{vmatrix} \begin{vmatrix} f_3(r) \\ g_3(r) \end{vmatrix} = 0, \tag{27d}$$

which are valid for the states $S_{3/2}$, $P_{1/2}$, $P_{3/2}$, and $P_{5/2}$, respectively. The differential equation for $P_{1/2}$ states (27b) can be solved exactly because it is similar to a hydrogenlike radial equation for p states, and we find that its eigenvalues are

$$E(nP_{1/2}) = \frac{1}{(1+\mu)n^2} \quad (n=2,\ 3,\ \ldots). \tag{28}$$

Exact solutions of the Hamiltonians for the $S_{3/2}$, $P_{3/2}$, and $P_{5/2}$ states have not been found. Approximate solutions of these Hamiltonians obtained using the variational method will be discussed in Sec. IV.

B. Weak Spin-Orbit Coupling

The acceptor Hamiltonian valid in this limit is (19) and the total angular momentum $\vec{F}=\vec{L}+\vec{I}$ is again a constant of motion. Also in this case the spin-orbit term couples only hydrogenic states for which $\Delta L = 0, \pm 2$. In the L-I coupling scheme the hydrogenic nS states give rise only to nS_1 states, while the hydrogenic nP states split into nP_0, nP_1, and nP_2. The most general functions describing these states are

$$\Phi(S_1) = F_0(r)\,|L=0,\ I=1,\ F=1,\ F_z\rangle + G_0(r)\,|L=2,\ I=1,\ F=1,\ F_z\rangle, \tag{29a}$$

$$\Phi(P_0) = F_1(r)\,|L=1,\ I=1,\ F=0,\ F_z\rangle, \tag{29b}$$

$$\Phi(P_1) = F_2(r)\,|L=1,\ I=1,\ F=1,\ F_z\rangle, \tag{29c}$$

$$\Phi(P_2) = F_3(r)\,|L=1,\ I=1,\ F=2,\ F_z\rangle + G_3(r)\,|L=3,\ I=1,\ F=2,\ F_z\rangle. \tag{29d}$$

The matrix elements of the acceptor Hamiltonian (19) between the above functions can be calculated using expressions (25) and (26). The values of the reduced matrix elements appropriate for this case are given in the Appendix. As a result we find the following systems of differential equations for the radial wave functions $F_i(r)$ and $G_i(r)$:

$$\begin{vmatrix} \frac{d^2}{dr^2}+\frac{2}{r}\frac{d}{dr}+\frac{2}{r}-E & -\sqrt{2}\,\mu\left(\frac{d^2}{dr^2}+\frac{5}{r}\frac{d}{dr}+\frac{3}{r^2}\right) \\ -\sqrt{2}\,\mu\left(\frac{d^2}{dr^2}-\frac{1}{r}\frac{d}{dr}\right) & (1+\mu)\,\frac{d^2}{dr^2}+\frac{2}{r}\frac{d}{dr}-\frac{6}{r^2}+\frac{2}{r}-E \end{vmatrix} \begin{vmatrix} F_0(r) \\ G_0(r) \end{vmatrix} = 0, \tag{30a}$$

$$\left[(1+2\mu)\left(\frac{d^2}{dr^2}+\frac{2}{r}\frac{d}{dr}-\frac{2}{r^2}\right)+\frac{2}{r}-E\right] F_1(r) = 0, \tag{30b}$$

$$\left[(1-\mu)\left(\frac{d^2}{dr^2}+\frac{2}{r}\frac{d}{dr}-\frac{2}{r^2}\right)+\frac{2}{r}-E\right] F_2(r) = 0, \tag{30c}$$

$$\begin{vmatrix} (1+\frac{1}{5}\mu)\left(\frac{d^2}{dr^2}+\frac{2}{r}\frac{d}{dr}-\frac{2}{r^2}\right)+\frac{2}{r}-E & \frac{3}{5}\sqrt{6}\,\mu\left(\frac{d^2}{dr^2}+\frac{7}{r}\frac{d}{dr}+\frac{8}{r^2}\right) \\ \frac{3}{5}\sqrt{6}\,\mu\left(\frac{d^2}{dr^2}-\frac{3}{r}\frac{d}{dr}+\frac{3}{r^2}\right) & (1+\frac{4}{5}\mu)\left(\frac{d^2}{dr^2}+\frac{2}{r}\frac{d}{dr}-\frac{12}{r^2}\right)+\frac{2}{r}-E \end{vmatrix} \begin{vmatrix} F_3(r) \\ G_3(r) \end{vmatrix} = 0, \tag{30d}$$

which apply to the states S_1, P_0, P_1, and P_2, respectively. The differential equations (30b) for the P_0 states and (30c) for the P_1 states are similar to hydrogenlike radial Hamiltonians for p states and can be solved exactly. The corresponding eigenvalues are

$$E(nP_0)=\frac{1}{(1+2\mu)n^2} \quad (n=2,\ 3,\ \ldots) \tag{31}$$

and

$$E(nP_1)=\frac{1}{(1-\mu)n^2} \quad (n=2,\ 3,\ \ldots). \tag{32}$$

Approximate variational solutions to the Hamiltonians for the S_1 and P_2 states will be discussed in Sec. IV.

IV. METHOD OF SOLUTION AND RESULTS

Exact solutions for the eigenvalues and the eigenfunctions of the radial acceptor Hamiltonians (27) and (30) are in general very hard to obtain. Only for the $P_{1/2}$, P_0, and P_1 states can an exact solution be obtained since, in these cases, the Hamiltonian reduces to that of the hydrogen atom for p states. For the other states, we have solved each Hamiltonian using the variational technique. We have assumed as trial wave functions, superpositions of Gaussian functions times the lowest possible polynomials which behave correctly at the origin.[9] For the $S_{3/2}$ state we have used

$$f_0(r)=\sum_{i=1}^{21} A_i e^{-\alpha_i r^2} \tag{33a}$$

and

$$g_0(r)=r\sum_{i=1}^{21} B_i e^{-\alpha_i r^2}. \tag{33b}$$

The same trial wave functions have also been used for the variational solution of the S_1 radial Hamiltonian (30a). Similarly, the trial wave functions used for the $P_{3/2}$ state,

$$f_2(r)=r\sum_{i=1}^{21} C_i e^{-\alpha_i r^2} \tag{34a}$$

and

$$g_2(r)=r^2\sum_{i=1}^{21} D_i e^{-\alpha_i r^2}, \tag{34b}$$

have also been used to approximate the radial part of the $P_{5/2}$ and P_2 eigenfunctions. While the linear parameters A_i, B_i, C_i, and D_i were used as variational parameters in order to minimize the energy, the same constant set of values for the 21 parameters α_i was used throughout the calculations. These parameters have been chosen in geometrical progression ($\alpha_{i+1}=g\alpha_i$, with g independent of i) and their range of values is wide enough to cover all actual situations met in studying the acceptor spectrum, the smallest value being $\alpha_1=1\times10^{-2}$ and the largest $\alpha_{21}=5\times10^5$. For example, with this set of Gaussian functions, the lowest-energy eigenvalues of the hydrogen atom for s and p symmetries are $E(1s)=1.00000$, $E(2s)=0.24999$, $E(2p)=0.25000$, and $E(3p)=0.10889$, in units of R_0.

The energies of the lowest acceptor states of interest are tabulated as a function of μ in Tables III and IV for the cases of strong and weak spin-orbit interaction, respectively. The energy spectrum for the more relevant case of strong spin-orbit coupling is also given in Fig. 3. These results represent the first extensive theoretical investigation of the acceptor energy spectrum as function of the valence-band parameters. An interesting feature of these two energy spectra is the

TABLE III. Acceptor energy spectrum as function of the parameter μ in the strong spin-orbit limit ($\bar{\Delta}=\infty$). The energies are in units of the effective Rydberg R_0.

μ	$1S_{3/2}$	$2S_{3/2}$	$2P_{1/2}$	$2P_{3/2}$	$2P_{5/2}$
0.00	1.000	0.250	0.250	0.250	0.250
0.05	1.002	0.251	0.238	0.261	0.248
0.10	1.009	0.254	0.227	0.273	0.248
0.15	1.021	0.258	0.217	0.287	0.249
0.20	1.037	0.264	0.208	0.302	0.251
0.25	1.060	0.273	0.200	0.320	0.256
0.30	1.089	0.284	0.192	0.341	0.262
0.35	1.125	0.297	0.185	0.365	0.270
0.40	1.171	0.313	0.179	0.394	0.281
0.45	1.228	0.333	0.172	0.428	0.295
0.50	1.299	0.358	0.167	0.468	0.322
0.55	1.388	0.388	0.161	0.518	0.336
0.60	1.503	0.426	0.156	0.580	0.366
0.65	1.653	0.476	0.152	0.660	0.406
0.70	1.857	0.542	0.147	0.767	0.461
0.75	2.145	0.635	0.143	0.917	0.539
0.80	2.580	0.773	0.139	1.142	0.657
0.85	3.309	1.003	0.135	1.518	0.857
0.90	4.768	1.460	0.132	2.268	1.259
0.95	9.145	2.820	0.128	4.521	2.470
1.00	∞	∞	0.125	∞	∞

TABLE IV. Acceptor energy spectrum as function of the parameter μ in the weak spin-orbit limit ($\bar{\Delta}=0$). The energies are in units of the effective Rydberg R_0.

μ	$1S_1$	$2P_0$	$2P_1$	$2P_2$
0.00	1.000	0.250	0.250	0.250
0.05	1.004	0.227	0.263	0.249
0.10	1.017	0.208	0.278	0.251
0.15	1.037	0.192	0.294	0.255
0.20	1.064	0.179	0.313	0.261
0.25	1.100	0.167	0.333	0.269
0.30	1.145	0.156	0.357	0.281
0.35	1.201	0.147	0.384	0.295
0.40	1.268	0.139	0.417	0.312
0.45	1.351	0.132	0.455	0.333
0.50	1.453	0.125	0.500	0.360
0.55	1.580	0.119	0.556	0.393
0.60	1.742	0.114	0.625	0.435
0.65	1.952	0.109	0.714	0.490
0.70	2.234	0.104	0.833	0.565
0.75	2.631	0.100	1.000	0.669
0.80	3.228	0.096	1.250	0.827
0.85	4.227	0.093	1.667	1.091
0.90	6.224	0.089	2.500	1.619
0.95	12.213	0.086	5.000	3.207
1.00	∞	0.083	∞	∞

diverging binding energy of a few levels (and the ground state among them) when μ approaches 1. This behavior is consistent with the valence-band dispersion relation (14), which shows that for $\mu=1$ one valence band becomes flat and therefore gives rise to infinite binding energy in a Coulomb potential. The same is also valid in the case of weak spin-orbit coupling. Not all levels however have diverging binding energy for $\mu=1$. These levels ($P_{1/2}$ and P_0), which have finite binding energy at $\mu=1$, are associated with those valence bands that maintain their parabolic behavior at $\mu=1$ and therefore do not give rise to any extreme localization. These two classes of acceptor states have different behavior not only for μ approaching 1 but also over the entire range of μ. In fact divergent levels have increasing binding energy for increasing μ while the opposite behavior is valid for nondivergent levels.

When μ increases, we observe not only an increase in binding energy but also a localization of the wave function. This is evident from Fig. 4, where the radial functions $f_0(r)$ and $g_0(r)$ of the ground state $1S_{3/2}$ are shown for different values of μ. A measure of the localization of the wave functions is given by the expectation value $\langle r\rangle$ over the various acceptor states. This quantity is shown in Fig. 5. As expected, all states become more localized when μ increases, with the only exception the state $P_{1/2}$, which shows the opposite behavior. From the ground-state radial functions

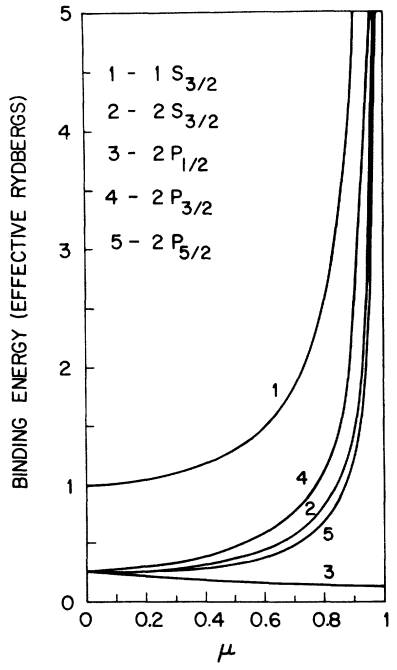

FIG. 3. Calculated acceptor energy spectrum as a function of μ in the strong spin-orbit coupling limit ($\bar{\Delta}=\infty$). The cubic term has been neglected ($\delta=0$). The energies are in units of the effective Rydberg R_0.

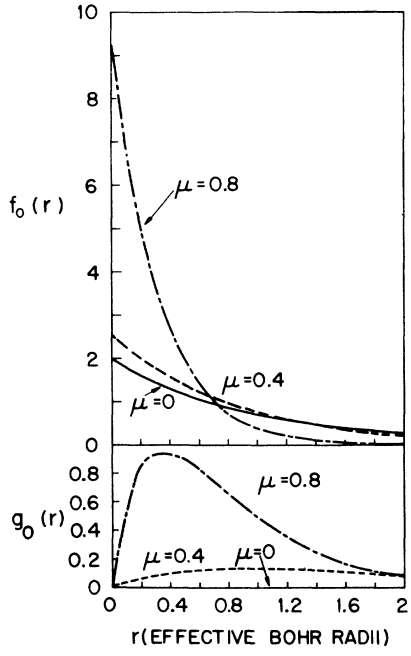

FIG. 4. Radial wave functions $f_0(r)$ and $g_0(r)$ of the acceptor ground state for different values of μ. Note the increase in localization and the increase in the g_0 component as μ increases. The functions are normalized in such a way that $\int_0^\infty[|f_0|^2+|g_0|^2]r^2dr=1$ and are given in units of $a_0^{-3/2}$, a_0 being the effective Bohr radius.

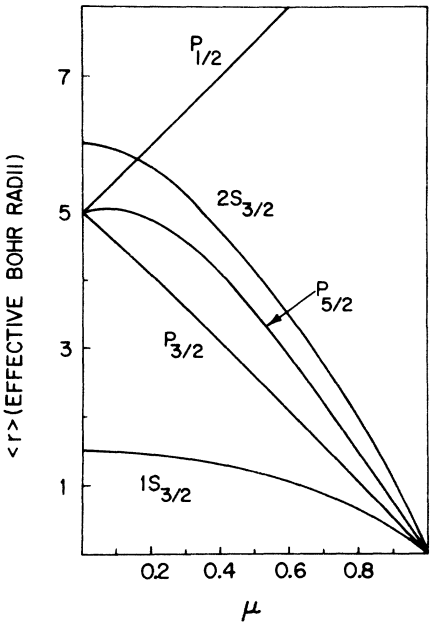

FIG. 5. Expectation value of r for various acceptor state as a function of μ. While $\langle r \rangle$ increases with μ for the state $P_{1/2}$, all other states become more localized as μ increases and have $\langle r \rangle = 0$ for $\mu = 1$.

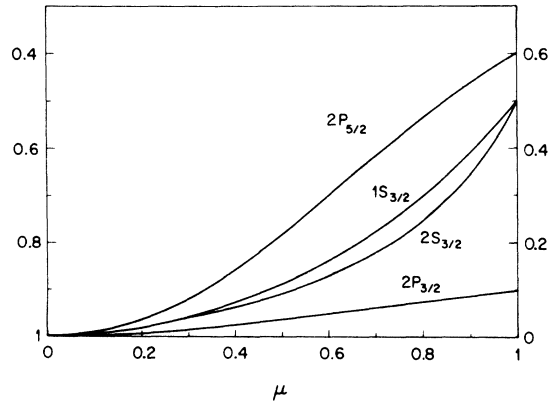

FIG. 6. Admixture coefficients of different *orbital* angular momenta as function of μ for the acceptor states studied in the present paper. The left scale refers to the lower orbital angular momentum (f_l functions) and the right scale refers to the higher orbital angular momentum (g_l functions). The g components increase with μ as is also shown for the ground state in Fig. 4. The state $2P_{1/2}$ is not shown because it has only a single orbital angular momentum component.

given in Fig. 4 we see that localization is not the only effect occurring for increasing μ. The admixture of different orbital angular momenta also changes appreciably with μ. The change with μ of the admixture probabilities is shown in Fig. 6 for the various acceptor states.

A quantity of interest when estimating central-cell corrections is the probability of finding the trapped hole at the impurity site. This probability is given in Table V as a function of μ for the two lowest states that do not vanish at the origin, i.e., $1S_{3/2}$ and $2S_{3/2}$. The result that these probabilities increase with μ is rather obvious and is a direct consequence of the localization effect previously mentioned. However, the ratio of the two probabilities for the same value of μ is surprisingly nearly constant over the complete range of μ and very close to its hydrogenic value of 8. An estimate of the importance of central-cell corrections can also be obtained from Table VI, where we give the theoretical acceptor spectra in the spherical approximation together with available experimental values of the acceptor ionization energies. We note that the comparison between theory and experiment is somewhat doubtful for those crystals, like Si and GaP, where the strength of the cubic term in the acceptor Hamiltonian is relatively high. Furthermore we wish to mention that the spherical-model acceptor spectra in Si and Ge are in satisfactory agreement with previous theoretical energy spectra.[8-11]

Up to now we have considered the acceptor energy spectrum in the two extreme limits of strong ($\bar{\Delta} = \infty$) and weak ($\bar{\Delta} = 0$) spin-orbit coupling, when $\bar{\Delta}$ is the spin-orbit splitting in the valence bands at the center of the Brillouin zone measured in units of the effective Rydberg, Eq. (9). While in most cases considered in Table VI the acceptor binding energy is much smaller than the spin-orbit splitting and therefore the result for $\bar{\Delta} = \infty$ are a reasonable approximation, in some cases it may be necessary to evaluate the acceptor energy spectrum for finite values of $\bar{\Delta}$. Under these circumstances the acceptor Hamiltonian becomes a 6×6 matrix operator and its solution is rather intricate. An approximate way to obtain the effects of a finite value of $\bar{\Delta}$ is to interpolate between the values obtained

TABLE V. Probability of finding the acceptor hole at the impurity site as a function of the valence-band parameter μ for the states $1S_{3/2}$ and $2S_{3/2}$ in the strong spin-orbit coupling limit. This probability can be used to estimate central-cell corrections and is given in units of $(4\pi a_0^3)^{-1}$, a_0 being the effective Bohr radius.

μ	$1S_{3/2}$	$2S_{3/2}$	μ	$1S_{3/2}$	$2S_{3/2}$
0.0	4.00	0.50	0.6	15.2	1.9
0.1	4.12	0.51	0.7	30.0	3.9
0.2	4.52	0.56	0.8	85.2	11.3
0.3	5.30	0.66	0.9	576.6	77.7
0.4	6.74	0.84	1.0	∞	∞
0.5	9.46	1.20			

TABLE VI. Theoretical energy spectrum of acceptor impurities in the strong spin-orbit coupling limit as predicted by the spherical model using the parameters given in Table I. Experimental ionization energies are also given. The symbols in parentheses refer to the kind of impurity and the energy unit is meV.

	E_i(expt.)	$1S_{3/2}$	$2S_{3/2}$	$2P_{1/2}$	$2P_{3/2}$	$2P_{5/2}$
Si	68.9[a](Al)	31.6	8.6	4.2	11.2	7.6
Ge	10.8[b](Ga)	9.8	2.9	0.6	4.2	2.5
AlSb	33[c] (?)	42.4	12.4	3.3	17.5	10.5
GaP	64.0[d](Zn)	47.5	13.7	4.2	19.1	11.7
GaAs	31.0[e](Zn)	25.6	7.6	1.6	11.1	6.5
GaSb	$13 \approx 15$[f](Si?)	12.5	3.8	0.65	5.6	3.2
InP	56.3[g](Cd)	35.2	10.5	2.0	15.5	8.9
InAs		16.6	5.1	0.4	7.9	4.4
InSb	~10[h] (Cd)	8.6	2.7	0.2	4.2	2.3
ZnS		175.6	52.0	11.7	75.1	44.1
ZnSe	114[i] (Li)	110.1	33.0	6.1	48.6	28.0
ZnTe		77.7	23.0	5.1	33.4	19.6
CdTe		87.4	26.5	3.7	39.9	22.6

[a]A. Onton, P. Fisher, and A. K. Ramdas, Phys. Rev. 163, 686 (1967).

[b]R. L. Jones and P. Fisher, J. Phys. Chem. Solids 26, 1125 (1965).

[c]R. J. Stirn and W. M. Becker, Phys. Rev. 148, 907 (1966); B. T. Ahlburn and A. K. Ramdas, Phys. Rev. 187, 932 (1969).

[d]P. J. Dean, R. A. Faulkner, S. Kimura, and M. Ilegems, Phys. Rev. B 4, 1926 (1971).

[e]W. Schairer and T. O. Yep, Solid State Commun. 9, 421 (1971).

[f]I. I. Burdiyan, S. B. Mal'tsev, I. F. Mironov, and Yu. G. Schreter, Fiz. Tekh. Poluprovodn. 5, 1996 (1971) [Sov. Phys.-Semicond. 5, 1734 (1972)].

[g]A. M. White, P. J. Dean, K. M. Fairhurst, W. Bardsley, E. W. Williams, and B. Day (unpublished).

[h]R. Kaplan (private communication).

[i]J. L. Merz, K. Nassau, and J. W. Shiever (unpublished).

for $\bar{\Delta}=0$ and for $\bar{\Delta}=\infty$. For the state $1S_{3/2}$ and $2S_{3/2}$ such interpolation can be conveniently done with the functions $S_1(\bar{\Delta})$ and $S_2(\bar{\Delta})$, respectively, which we have defined in our investigation of the exciton energy spectrum.[15] The functions $S_1(\bar{\Delta})$ and $S_2(\bar{\Delta})$ are the exact interpolating functions for the case in which the terms in μ, δ, and $\bar{\Delta}$ can be handled in perturbation theory, and therefore we expect them to be a reasonable approximation even in our case. The effect of finite $\bar{\Delta}$ is particularly significant in the case of Si. In this case the interpolation to finite $\bar{\Delta}$ for the state $1S_{3/2}$ is shown in Fig. 7. We see that even in the case of Si this effect is relatively small, and therefore we believe that the approximate interpolation scheme here proposed is accurate enough for most practical purposes.

Having studied the energy spectrum of Hamiltonian (12) for all positive values of $\mu \leq 1$, we are now in a better position to discuss analogies and differences between the acceptor problem and the direct exciton problem. We have already seen that the two systems are described by the same Hamiltonian, the only difference being in the strength of the "spin-orbit" terms which for the exciton case are scaled by a factor $\alpha \approx 0.3$. This means that the strength of the "spin-orbit" terms is $\mu \approx 0.7$ for acceptors and $\mu' = \alpha\mu \approx 0.2$ for excitons. These two values of μ correspond to completely different regions as is shown in Fig. 8. In the exciton regime (small μ) the spin-orbit terms can be treated using perturbation theory and the energy spectrum deviates only slightly from that of the hydrogen atom. In the acceptor regime (μ close to 1) the spin-orbit terms produce such an extreme localization of the acceptor wave functions that the energy spectrum has no resemblance at all with that of the hydrogen atom. This effect is due to the fact that one of the valence bands becomes flat in the limit $\mu \to 1$.

V. CONCLUSIONS

We have studied the problem of shallow acceptor states in semiconductors using a spherical model in which the generally small cubic terms that appear in the acceptor Hamiltonian are completely neglected. The model gives a reasonably good approximation to the acceptor energy spectra in most semiconductors and reduces the formidable acceptor Hamiltonian to simple radial differential equations which have been solved with the variational technique. Though the model, as it is, is

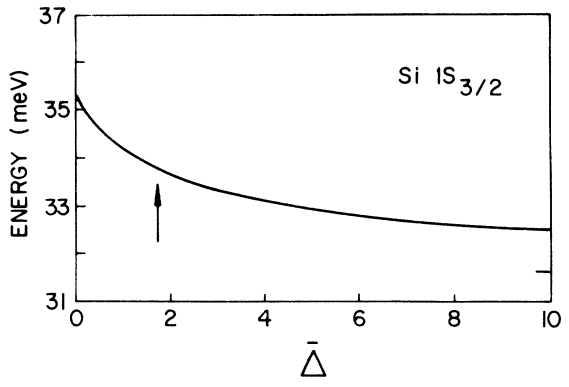

FIG. 7. Variation of the ground-state ionization energy in Si with the valence-band spin-orbit splitting $\bar{\Delta}$ (in units of the effective Rydberg R_0). The ionization energy for intermediate values of $\bar{\Delta}$ has been obtained by interpolating between the limits of strong and weak spin-orbit coupling with the function appropriate for the ground state of the exciton. The arrow corresponds to the actual value of $\bar{\Delta}$ in Si and gives an ionization energy of 33.7 meV. The horizontal mark on the right side corresponds to the ionization energy for $\bar{\Delta}=\infty$, which is 31.6 meV.

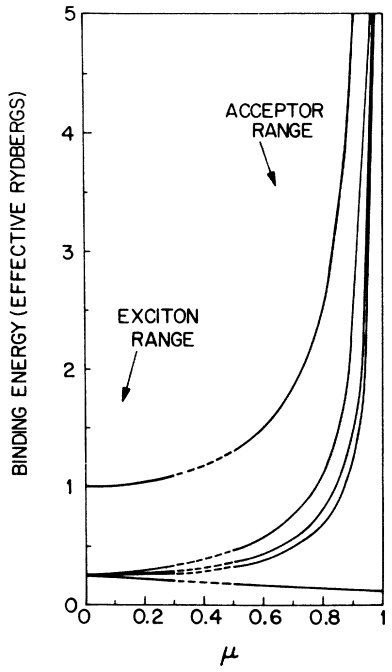

FIG. 8. Exciton problem and acceptor problem are described by the same formal Hamiltonian but have completely different energy spectra. The figure shows the appropriate range of μ values for excitons and acceptors. While for excitons the effect of μ can be treated by perturbation theory and the energy spectrum is nearly hydrogenic, the situation is completely different for acceptors.

generally satisfactory, various improvements can be made to it. First of all, the cubic terms which are responsible for energy shifts and splittings in the energy spectrum can be included.[13] This improvement is presently under investigation and will be the subject of a future publication.[16] Acceptor energy spectra accurate to 10^{-3} eV will also require a more accurate treatment of the effects of the finite value of the spin-orbit splitting than the approximate interpolation technique proposed in the present paper. Finally, in the case of zinc-blende crystals, one should also consider the corrections to the binding energy produced by the terms which are linear in the hole momentum. The effects of these terms, which we have neglected, can be studied in the framework of the spherical model.

The problem of acceptor states also requires a detailed study of the acceptor potential. In the present paper we have studied the problem using a screened Coulomb potential and we have neglected short-range potentials which are due to the impurity core and which are responsible for the chemical shifts of the acceptor energy levels. A step forward in the understanding of the short-range component of the impurity potentials has recently been taken by Baldereschi and Hopfield[19] in connection with the problem of isoelectronic traps, but much work has still to be done in this direction.

Furthermore we wish to mention that the spherical model is an excellent starting point for the study of the effects on the acceptor spectrum due to external perturbations such as magnetic fields and strain fields. Since external perturbations are a powerful tool for the experimental investigation of acceptor states only when a detailed theoretical treatment of their effects is available, work must be done also in this direction and the spherical model will be of valuable help.

APPENDIX

In this Appendix we briefly review the results of angular momentum theory which have been used in the present study of the acceptor Hamiltonian. These results will be given without proof, which can be found, for example, in the book by Edmonds.[18]

A given Cartesian tensor of second rank T_{ik}, where $i, k = 1, 2, 3$ means x, y, and z, respectively, can always be reduced to irreducible spherical tensors of rank 0, 1, and 2 as follows:

$$T_0^{(0)} = T_{11} + T_{22} + T_{33} \quad \text{(rank 0)}, \tag{A1}$$

$$\left.\begin{aligned} T_0^{(1)} &= T_{12} - T_{21} \\ T_{\pm 1}^{(1)} &= \mp (1/\sqrt{2})[T_{23} - T_{32} \pm i(T_{31} - T_{13})] \end{aligned}\right\} \text{(rank 1)}, \tag{A2}$$

and

$$\left.\begin{aligned} T_0^{(2)} &= \sqrt{\tfrac{3}{2}}\, T_{33} \\ T_{\pm 1}^{(2)} &= \mp (T_{13} \pm i T_{23}) \\ T_{\pm 2}^{(2)} &= \tfrac{1}{2}(T_{11} - T_{22} \pm 2i T_{12}) \end{aligned}\right\} \text{(rank 2)}, \tag{A3}$$

where the quantization axis has been assumed to be the z axis or 3 axis. From the above definitions, it is evident that our tensors P_{ik}, J_{ik}, and I_{ik}, which are symmetric tensors with vanishing trace, can be decomposed only into irreducible spherical tensors of rank 2 according to formulas (A3).

Two spherical tensors of rank k_1 and k_2 can be coupled to form other spherical tensors whose rank k is limited by the condition $|k_1 - k_2| \le k \le (k_1 + k_2)$. The resulting spherical tensors are defined as

$$[T^{(k_1)} \times U^{(k_2)}]_q^{(k)} = (-1)^{k_1 - k_2 + q}(2k+1)^{1/2} \times \sum_{q_1, q_2} \begin{pmatrix} k_1 & k_2 & k \\ q_1 & q_2 & -q \end{pmatrix} T_{q_1}^{(k_1)} U_{q_2}^{(k_2)} . \tag{A4}$$

The values of the 3-j symbol $\left(\begin{smallmatrix} k_1 & k_2 & k \\ q_1 & q_2 & -q \end{smallmatrix}\right)$ have been tabulated by Rotenberg *et al.*[20] for the lowest values of the parameters. A special case of the product (A4) is obtained when $k_1 = k_2$ and $k = 0$. This special

case is the scalar product between tensors and is defined as

$$(T^{(k)}\cdot U^{(k)})=\sum_q (-1)^q T_q^{(k)} U_{-q}^{(k)} . \tag{A5}$$

Products of tensor operators have been used in the present paper to write the acceptor Hamiltonians in more convenient form. In this respect, the following reduction formulas will be useful:

$$\begin{aligned}(p_x^2J_x^2+p_y^2J_y^2+p_z^2J_z^2)&=\tfrac{1}{3}p^2J^2+\tfrac{2}{45}(P^{(2)}\cdot J^{(2)})\\&+\tfrac{1}{18}\{[P^{(2)}\times J^{(2)}]^{(4)}_{-4}\\&+\tfrac{1}{5}\sqrt{70}[P^{(2)}\times J^{(2)}]^{(4)}_{0}+[P^{(2)}\times J^{(2)}]^{(4)}_{4}\}\end{aligned} \tag{A6}$$

and

$$\begin{aligned}&\{p_xp_y\}\{J_xJ_y\}+\{p_yp_z\}\{J_yJ_z\}+\{p_zp_x\}\{J_zJ_x\}\\&=\tfrac{1}{30}(P^{(2)}\cdot J^{(2)})-\tfrac{1}{36}\{[P^{(2)}\times J^{(2)}]^{(4)}_{-4}\\&+\tfrac{1}{5}\sqrt{70}[P^{(2)}\times J^{(2)}]^{(4)}_{0}+[P^{(2)}+J^{(2)}]^{(4)}_{4}\},\end{aligned} \tag{A7}$$

where $\{ab\}=(ab+ba)/2$. Expressions (A6) and (A7) remain valid if the spin operator J is replaced by I.

Finally the matrix elements of the scalar product $(P^{(2)}\cdot J^{(2)})$ between eigenstates of the total angular momentum $\vec{F}=\vec{L}+\vec{J}$ are easily evaluated using the "reduced-matrix-element" technique, expression (25), which expresses the matrix element $\langle L', J, F, M|(P^{(2)}\cdot J^{(2)})|L, J, F, M\rangle$ in terms of a 6-j symbol and of the reduced matrix elements $(J||J^{(2)}||J)$ and $(L'||P^{(2)}||L)$. The values of the 6-j symbols can be found in the book by Rotenberg *et al.*[20] The reduced matrix elements are given by

$$(L-2||P^{(2)}||L)=-3\hbar^2\left(\frac{L(L-1)}{2L-1}\right)^{1/2}\times\left(\frac{d^2}{dr^2}+\frac{2L+1}{r}\frac{d}{dr}+\frac{L^2-1}{r^2}\right), \tag{A8}$$

$$(L||P^{(2)}||L)=\sqrt{3}\,\hbar^2\left(\frac{L(2L+1)(2L+2)}{(2L-1)(2L+3)}\right)^{1/2}\times\left(\frac{d^2}{dr^2}+\frac{2}{r}\frac{d}{dr}-\frac{L(L+1)}{r^2}\right), \tag{A9}$$

$$(L+2||P^{(2)}||L)=-\tfrac{3}{2}\hbar^2\left(\frac{(2L+2)(2L+4)}{2L+3}\right)^{1/2}\times\left(\frac{d^2}{dr^2}-\frac{2L+1}{r}\frac{d}{dr}+\frac{L(L+2)}{r^2}\right), \tag{A10}$$

$$(L'||P^{(2)}||L)=0 \text{ if } |L'-L|\neq 0, 2, \tag{A11}$$

$$(J||J^{(2)}||J)=\tfrac{1}{2}\sqrt{\tfrac{3}{2}}\times[(2J-1)(2J)(2J+1)(2J+2)(2J+3)]^{1/2}. \tag{A12}$$

---

*Present address: Ecole Polytechnique Federale Laboratoire de Physique Applique, Lausanne, Switzerland.

[1]W. Kohn, *Solid State Physics*, edited by F. Seitz and D. Turnbull (Academic, New York, 1957), Vol. 5, p. 257.

[2]C. Kittel and A. H. Mitchell, Phys. Rev. 96, 1488 (1954).

[3]J. M. Luttinger and W. Kohn, Phys. Rev. 97, 869 (1955).

[4]For a recent review on impurity states see J. C. Phillips, *Bonds and Bands in Semiconductors* (Academic, New York, 1973), Chap. 9.

[5]See, for example, M. L. Cohen and T. K. Bergstresser, Phys. Rev. 141, 789 (1966).

[6]W. Kohn and J. M. Luttinger, Phys. Rev. 98, 915 (1955).

[7]R. A. Faulkner, Phys. Rev. 184, 713 (1969).

[8]W. Kohn and D. Schecter, Phys. Rev. 99, 1903 (1955); D. Schecter, J. Phys. Chem. Solids 23, 237 (1962).

[9]K. S. Mendelson and H. M. James, J. Phys. Chem. Solids 25, 729 (1964).

[10]K. Suzuki, M. Okazaki, and H. Hasegawa, J. Phys. Soc. Japan 19, 930 (1964).

[11]K. S. Mendelson and D. R. Schultz, Phys. Status Solidi 31, 59 (1969).

[12]V. I. Sheka and D. I. Sheka, Zh. Eksp. Teor. Fiz. 51, 1445 (1966) [Sov. Phys.-JETP 24, 975 (1967)].

[13]N. O. Lipari and A. Baldereschi, Phys. Rev. Lett. 25, 1660 (1970); N. O. Lipari and A. Baldereschi, in *Proceedings of the Eleventh International Conference on the Physics of Semiconductors*, Warsaw, 1972 (Polish Scientific, Warsaw, 1972).

[14]J. M. Luttinger, Phys. Rev. 102, 1030 (1956).

[15]A. Baldereschi and N. O. Lipari, Phys. Rev. B 3, 439 (1971).

[16]A. Baldereschi and N. O. Lipari (unpublished).

[17]J. Dresselhaus, J. Phys. Chem. Solids 1, 14 (1956).

[18]A. R. Edmonds, *Angular Momentum in Quantum Mechanics* (Princeton U. P., Princeton, N. J., 1960).

[19]A. Baldereschi and J. J. Hopfield, Phys. Rev. Lett. 28, 171 (1972).

[20]M. Rotenberg, R. Bivins, N. Metropolis, and J. K. Wooten, *The 3-j and 6-j Symbols* (Technology Press, Cambridge, Mass., 1959).